Formation of angular power profile via ballistic light transport in multimode optical fibers with corrugated surfaces

E. I. Chaikina, S. Stepanov, and A. G. Navarrete

División de Física Aplicada, Centro de Investigación, Científica y de Educación Superior de Ensenada, Apartado Postal 2732, Ensenada, Baja California, 22800 Mexico

E. R. Méndez*

Instituto de Física, Universidad Nacional Autónoma de México, Ciudad Universitaria, Apartado Postal 20-362, México Distrito Federal 01000, Mexico

T. A. Leskova

Department of Physics and Astronomy and Institute for Surface and Interface Science, University of California, Irvine, California 92697, USA

We present experimental results on the light transmission and intermode power exchange in multimode fibers with rough surfaces. The experiments were performed with chemically etched 200-μm-diameter cores of fused silica fibers that can support up to 700×700 guided modes at the wavelength employed, $\lambda \approx 0.6$ μm. After propagation through some rough fiber section the mode power profile acquires a Gaussian shape that propagates along the mean axis of the corrugated fiber, with a slowly reducing radius ($\propto 1/\sqrt{z}$), and practically without attenuation of the central intensity. These features, and other observed characteristics, are reproduced with a theory that assumes a ballistic regime of light propagation through a one-dimensional slab waveguide, relating the characteristic propagation lengths to parameters of the fiber surface roughness.

PACS number(s): 42.25.Dd, 72.15.Rn, 42.81.Dp

I. INTRODUCTION

The propagation and scattering of light in waveguides with bulk heterogeneities or corrugated walls have been topics of intensive fundamental and applied research for several decades. Originally this interest was motivated by the practical problem of assessing the light losses due to imperfections in integrated optical waveguides or optical fibers.[1–5] Investigations of this period (both experimental and theoretical) were generally concentrated on single-mode or multimode waveguides with a small number of guided modes, and were aimed at the evaluation of the light losses.

Later, the focus of research activity in this area switched to the more fundamental problem of light localization in disordered media.[6–9] It was understood that the transport of photons in such media can be an ideal model for studies of Anderson localization, and that random optical waveguides can be suitable objects for investigating related effects experimentally. Later different regimes of electromagnetic wave propagation were studied experimentally, through the observation of the statistics of microwaves propagating through hollow metal tubes with volume inhomogeneities.[10,11]

It has been shown theoretically[12,13] that, as far as their scattering properties are concerned, optical waveguide structures with bulk disorder are not equivalent to waveguides with surface disorder. In waveguides with bulk disorder, the efficiency of the intermode mixing does not depend on the mode index. On the other hand, in the case of surface roughness, the efficiency of the intermode mixing depends on the mode index dramatically, and different radiation transport behavior can be observed in the same waveguide.[14,15] Keep-

ing in mind this intriguing possibility, great efforts have been made recently on the theoretical analysis of the propagation of coherent light in multimode waveguides with corrugated walls.[16–19]

The theoretical papers mentioned above were, however, restricted to the case of slab waveguides with perfectly conducting walls with one-dimensional roughness. The experimental realization of such a system in the optical region of the spectrum is difficult, due to the attenuation that occurs in the reflection of light from real metals. Optical fibers, on the other hand, constitute a more natural system for optical experiments; they are easily available and have low intrinsic losses. In this paper, we report an experimental study on the propagation of light through multimode optical fibers with rough surfaces.

Some preliminary results on the power leakage of light through corrugated fiber walls followed by the formation of a narrow central peak in the angular distribution of the transmitted light in response to excitation by a rather broad initial profile were reported in Refs. 20 and 21. In the present paper, data on the formation of the Gaussian-shaped central peak are complemented with experimental results concerning the scattering and diffusion of the initially narrow angular light distributions employed for excitation. Discussion of these effects related basically to ballistic light propagation through the corrugated fiber is accompanied by a theoretical analysis. Particular attention is paid to the incoherent intermode power exchange between guided modes with low mode indices, which gives rise to the formation of the mentioned central peak. A detailed theoretical analysis and a discussion of the intermode power diffusion mechanisms that take place in corrugated optical fibers with high mode indices will be given elsewhere.[22]
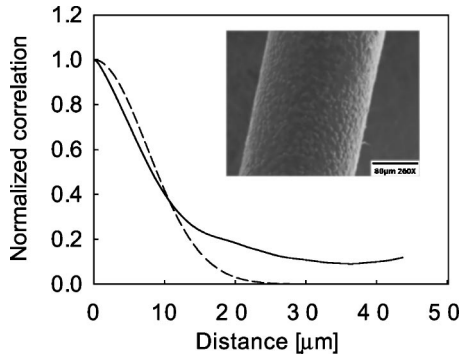
FIG. 1. Estimated correlation function of heights of the etched fiber surface (solid line). For reference, the dashed line shows a Gaussian correlation function with a $1/e$ correlation length a $=10$ μm. The inset shows a scanning electron microscope image of the fiber.

II. EXPERIMENTAL DETAILS AND RESULTS

As experimental samples we used fused silica ($n=1.457$) cores of multimode step index fibers (3M TECS™ FT-200-EMT) of diameter $d=200$ μm. The fiber cores were chemically etched to introduce the roughness (see inset of Fig. 1). The standard deviation of heights δ and the correlation length a of the surface roughness were estimated from profiles obtained with an electron scanning microscope and a DEKTAK3ST profilometer. A typical example of an estimated height correlation function is shown in Fig. 1. One can see that the correlation function is not a Gaussian function. In fact, the surface profile would be better modeled as a multiscale random process.[23] However, for the purpose of comparing our experimental results with theoretical predictions that employ a Gaussian height correlation model we define the correlation length a as the distance for which we have a $1/e$ decay in the correlation function. The estimated correlation lengths were in the range $4<a<12$ μm, and the standard deviation of heights (determined by the etching time) in the range $0.02<\delta<0.5$ μm.

In the experiments discussed below we used two sources of monochromatic coherent light: a single-mode cw semiconductor laser diode of wavelength $\lambda_1=655$ nm, and a He-Ne laser of wavelength $\lambda_2=633$ nm. To excite a broad and uniform angular spectrum of guided modes the input end of the fiber (still covered by the plastic cladding and jacket) was illuminated by a laser beam focused by a 40× microscopic objective [numerical aperture=0.65]. This allowed us to fill the entire angular aperture of the fiber (with numerical aperture=0.39), exciting about 250×250 transverse fiber modes. For comparison note that the clean fiber core without plastic cladding can support about 700×700 guided modes for the wavelengths used. To estimate the above numbers, we used the simple relation for the guided mode number in a one-dimensional (1D) slab waveguide.

The angular distribution of the light diverging from the output end of the etched section of the fiber was observed by a charge-coupled device (CCD) camera placed about 4 mm away from the fiber end. Alternatively, the far-field angular intensity distribution of the light emerging from the end of the fiber was measured with a scatterometer[23] (see Fig. 2).
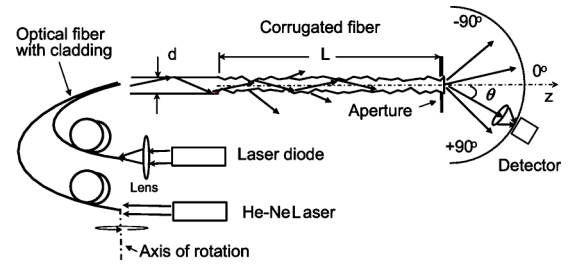
FIG. 2. Schematic diagram of the experimental setup used to measure the angular distribution of the light emerging from the end of the fiber.

The detection system, consisting of an aperture, a lens, and a silicon photodiode, had an effective detecting area of about 1 cm^2, and was placed about 1 m from the fiber end. This implied an averaging over approximately 7×7 neighboring modes, reducing the statistical fluctuations (speckle noise) in the measurements. In the scatterometer, the laser light was modulated with a chopper, and the output photodiode signal was processed with a lock-in amplifier. The light radiated from the sides of the etched fiber was blocked using baffles and apertures.

Figure 3 shows the normalized (to the central value) angular distribution of the output intensity $I_{out}(\theta,z)$ as a function of the lengths z of the etched section of a fiber with δ $=0.15$ μm. The length of the rough part of the fiber was sequentially reduced in these experiments by cutting off small pieces of the etched fiber. One can see from Fig. 3 that at the beginning of the etched piece, the angular light power distribution fills practically the whole numerical aperture of the fiber with the plastic cladding. As we mentioned earlier, the open fiber core supports a much larger number of guided modes. During their propagation along the fiber, the initially excited fiber modes are scattered from the rough fiber walls into other modes with higher or lower mode indices (i.e., propagation angles). After each collision with the rough fiber wall the mode typically changes its longitudinal wave number by some value approximately limited by the power spectrum half-width $\Delta k\approx2/a$ ($0.5-0.2$ μm^{-1} in our experiments). To fill the angular spectrum of the modes supported by the open core, several collisions of the initially excited modes with the rough walls are needed. One can see from
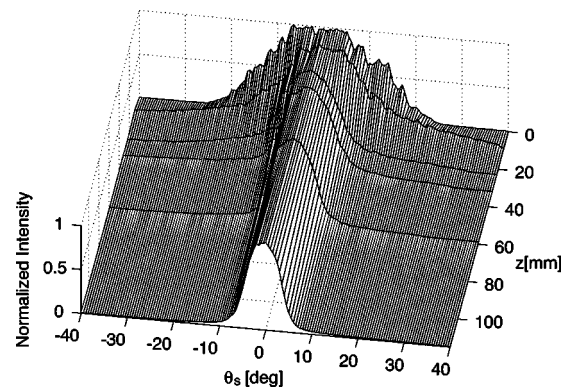
FIG. 3. Measurements of the far-field angular intensity distribution of the light transmitted through the fiber as a function of the length of the rough section.
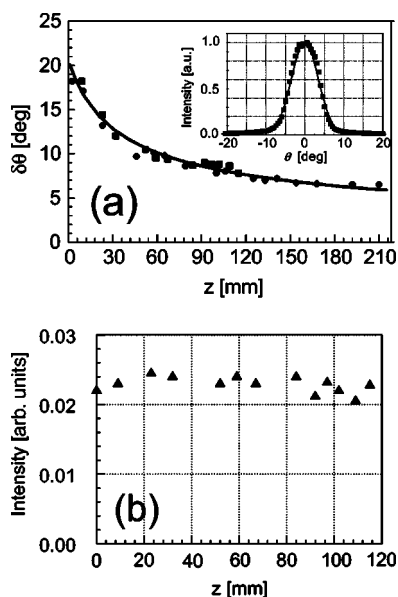
FIG. 4. (a) Half-width of the output angular distribution (see Fig. 3) as a function of the propagation lengths. The squares and circles correspond to data obtained with two different fiber samples with similar standard deviation of height. The solid line corresponds to an inverse square root dependence. The inset shows a typical profile formed after propagation through a relatively long (z = 115 mm) piece of corrugated fiber. The experimental data are denoted by the squares and the line represents a Gaussian function. (b) Intensity in the center of the output angular distribution as a function of the propagation length.

FIG. 5. Far-field angular intensity distributions excited at different angles of incidence θ_{in} of the laser beam used to feed the rough section of the fiber. The inset shows the 2D angular intensity distribution corresponding to $\theta_{in} = 15°$.

Fig. 3 that, after propagation through the first few millimeters of the etched fiber, some wings that correspond to higher-order modes appear in the output angular distribution. These guided modes, which have been excited through the roughness and have propagation angles close to the critical one, can escape from the fiber into the surrounding medium through subsequent scattering events. And indeed,[20] the formation of broad wings in the angular spectrum of propagating modes is accompanied by intensive radiation from the fiber sides.

Further propagation through the corrugated fiber reduces the half-width of the angular profile down to a value smaller than 0.2 rad. The wings in the angular profile lose their power significantly and that, in turn, reduces the power leakage. In this way, the light propagates with little attenuation through a relatively long length of the rough fiber (up to the maximum value of 210 mm used in our experiments). In this region, the width of the angular profile reduces slowly and has a practically constant central maximum (see Fig. 4). Note that, while the propagation through the initial centimeters of the etched fiber is characterized by a significant reduction of the transmitted power due to leakage through the fiber walls, the attenuation of the light propagating with this narrowed angular distribution is rather low. The central maximum formed in this way has a profile that is fitted by a Gaussian function quite well [see inset of Fig. 4(a)].

In another series of experiments we used narrow angular spectrum excitation. For this purpose, the input end of the fiber was illuminated with a collimated beam from a

He-Ne laser. By adjusting the angle of incidence on the input end of the fiber (θ_{in}) with the help of a rotating optical table, we could excite a limited number of modes with transverse wave numbers (i.e., angles of propagation) around the desired central value.[24] The inset of Fig. 5 shows a typical ring distribution of the power of the modes excited with $\theta_{in} \approx 15°$, as it is observed with a CCD camera at the end of the clean fiber. This kind of angular power profile is used to feed the rough section of the fiber. Similar input power distributions obtained with different incidence angles and measured using the scatterometer are shown in Fig. 5. One can see that the angular widths of the observed profiles are significantly larger than those solely due to diffraction at the fiber output aperture (d) and grow as the angle of incidence is decreased. We attribute this broadening to imperfections at the ends of the fiber (the faces were not polished) and also to an intermode mixing in the initial part of the fiber due to its coiling. The observed reduction in the maximum intensity of the profiles with an increase of the angle of incidence is due to the difference in the ring area (growing linearly with θ_{in}) through which the total introduced power is distributed.

Figure 6 shows the angular profiles of the output light intensity obtained for different lengths z of the etched part of the fiber for laser beam incidence angles $\theta_{in} \approx 5°$, 10°, and 15°. Even without a detailed analysis of these curves one can see that all the initial profiles finally evolve into Gaussian-like curves, similar to the one shown in the inset of Fig. 4.

III. THEORETICAL ANALYSIS

We start the theoretical analysis of the power transfer in the region of the central peak by considering a multimode 1D slab dielectric waveguide of thickness d and refractive index n [see Fig. 7(a)]. The two interfaces of the waveguide are assumed to have uncorrelated 1D roughness (i.e., there are height variations along the z axis only) with a Gaussian power spectrum:

$$g(\Delta k) = \sqrt{\pi} a k_0 \exp\left[-\left(\Delta k \frac{a k_0}{2}\right)^2\right]. \tag{1}$$

Here and below we use normalized (to the wave number of light in the surrounding space $k_0 = 2\pi/\lambda$) longitudinal k and
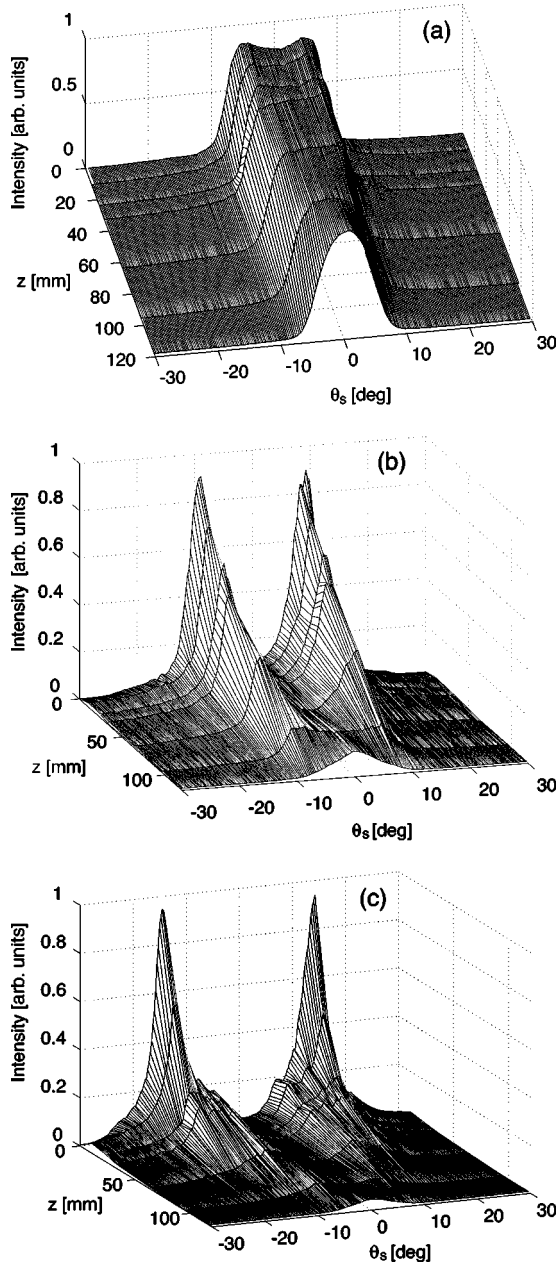
FIG. 6. Measurements of the far-field angular intensity distribution of the light transmitted through the fiber as a function of the length of the rough section for three different angles of incidence: (a) $\theta_{in}=5°$, (b) $10°$, and (c) $15°$.

transverse κ wave numbers of the guided modes [see Fig. 7(b)]. We also assume a simplified parabolic relation between the longitudinal and the transverse wave numbers:

$$\kappa^2 = n^2 - k^2 \approx 2n(n-k). \tag{2}$$

Note that the transverse wave number κ practically coincides with the angle θ at which this particular mode is radiated from the output waveguide end: $\theta = \arcsin(\kappa)$ ($\approx \kappa$ for $\theta \lesssim 0.5$). The waveguide under consideration is assumed to be multimode with a total number of modes $N = \kappa_{max}/(\pi/k_0 d) \gg 1$.
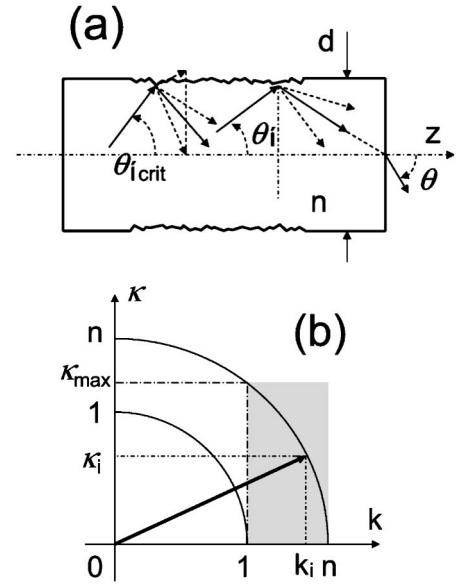
FIG. 7. (a) Intermode scattering and leakage of light via rough walls of 1D slab waveguide. (b) k-space representation of the ith guided mode.

We consider the transfer of power from some initial mode of index i into mode j after traversing a small section of rough fiber of length Δz. The transmission coefficient T_{ij} has been obtained for the case of corrugated metal walls.[24–26] Given our assumptions about the roughness spectrum, the probabilities associated with leakage and reflection are small. Then

$$T_{ij} = \Delta z \frac{2\delta^2 \kappa_i^2 \kappa_j^2}{d^2 k_i k_j} k_0 g(|k_i - k_j|). \tag{3}$$

This approximation is correct for a dielectric waveguide as long as the penetration depth into the surrounding medium can be neglected in comparison with the waveguide width d. Similarly, the transmission coefficient T_{ii}, which describes the attenuation of mode i (see, e.g., Ref. 17) is given by

$$T_{ii} = 1 - \sum_{j \neq i} T_{ij} = 1 - \frac{\Delta z}{l_i}. \tag{4}$$

In Eq. (4) l_i is the characteristic attenuation length of this particular mode. The value of l_i can be obtained in an analytical way if one assumes a quasicontinuous mode distribution with density,

$$\rho(k) = \frac{d k_0}{\pi} \sqrt{\frac{n}{2}} \frac{1}{\sqrt{n-k}}, \tag{5}$$

and substitutes, in Eq. (4), summation over all the jth modes by integration over the roughness power spectrum. For the guided modes that are not too close to the borders of the permitted k values in Fig. 7(b) (i.e., those in the interval $[1 + 2/k_0 a, n - 2/k_0 a]$) we obtain the following result:

$$l_i = \frac{nd}{4\delta^2 k_0^2 \kappa_i^2}. \tag{6}$$

On the other hand, a detailed consideration of the incoherent intermode light power transfer in a similar 1D waveguide[21,22,25] results in a diffusion-type partial differential equation for the power density $P(z,k)$, which is considered as a quasicontinuous function of κ in this analysis. Under the above assumptions and when written in terms of the transverse wave numbers κ this equation reduces to the rather simple form

$$\frac{\partial P(z,\kappa)}{\partial z} = \frac{\partial}{\partial \kappa}\left[\frac{\kappa}{L_D}\frac{\partial P(z,\kappa)}{\partial \kappa}\right]. \qquad (7)$$

Here the characteristic length

$$L_D = \frac{da^2}{4n\delta^2} \qquad (8)$$

gives a natural scale to all power transfer processes in this system. With some reasonable boundary conditions [$P(z,\kappa_{max})=0$, which represents an effective power leakage through the rough fiber walls, and $\partial P(z,0)/\partial\kappa=0$], Eq. (7) can easily be solved both analytically (by separation of variables) and numerically. This allows us to predict the evolution of any initial power profile $P(0,\kappa)$ in its propagation through the corrugated waveguide.

This differential equation, as well as the equation for the mode attenuation length l_i [Eq. (6)], is however, not valid for the boundary areas of the allowed k region. Indeed, when the distance $(n-k)$ from the border is approaching the half-width of the power spectrum ($\simeq 2/k_0 a$), the integration over $\Delta k = k_j - k_i$ throughout the interval $[-\infty, \infty]$ that gave us the simple results expressed by Eqs. (6) and (7) is not correct. The size of the boundary region of nearly coaxial modes becomes clear when it is expressed in terms of the transverse wave numbers κ. From Eq. (2) we find that the guided modes with

$$\kappa \lesssim \Delta\kappa' = \frac{2\sqrt{n}}{\sqrt{k_0 a}} \qquad (9)$$

are inside this boundary region. For the wavelength $\lambda \approx 0.6\ \mu m$, $n \approx 1.5$ and the correlation length $a \approx 5\ \mu m$ we have $\Delta\kappa' \approx 0.3$. That is, the angular radius of this boundary region in the far field is about 20°. In this region, the evaluation of the light power transfer requires a different approach, and thus we present a more precise evaluation of the mode attenuation length.

It follows from Eq. (4) that in the approximation of a quasicontinuous mode distribution, the exact value of the attenuation length l_i' for the guided mode with longitudinal wavenumber k_i from the boundary region (i.e., with $n \gtrsim k_i \gtrsim n-2/k_0 a$) equals

$$l_i' \approx \left[\int_{-\infty}^{n-k_i} d(\Delta k)\rho(k_i + \Delta k)\right.$$

$$\left.\times \frac{8\delta^2 k_0(n-k_i)[n-(k_i+\Delta k)]}{d^2}g(|\Delta k|)\right]^{-1}. \qquad (10)$$

In contrast with Eq. (4), the summation over all possible final modes with $k_j = k_i + \Delta k$ is replaced here by integration with a
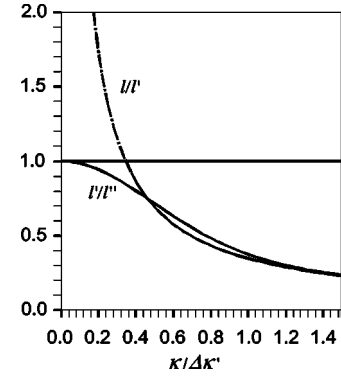
FIG. 8. Mode attenuation lengths l calculated for the internal part of the allowed k region (dashed line) and l' calculated taking into account the boundary effect (solid line). Both are normalized to the attenuation length l'', calculated in the approximation of nearly coaxial modes ($n-k \ll 2/a\kappa_0$).

density of modes in the final state $\rho(k_i + \Delta k)$ over Δk within the limits $[-\infty, n-k_i]$. We also used the approximate form of the parabolic equation [Eq. (2)] to obtain the transmission coefficients

$$T_{ij} \approx \Delta z \frac{8\delta^2 k_0(n-k_i)(n-k_j)}{d^2}g(|\Delta k|). \qquad (11)$$

In the evaluation of this general form of the attenuation length l_i', the fact that the deviation from the coaxial mode (i.e., that with $k \to n$) is small constitutes a useful approximation. Formally this means that everywhere in Eqs. (10) and (11) we replace k_i by n (except, of course, for a general multiplicative factor $n-k_i$). Direct integration gives us the following result for this particular case:

$$l_i'' = \frac{d\sqrt{\pi n}\sqrt{a}}{4\Gamma(3/4)\delta^2 k_0^{3/2}\kappa_i^2} = \frac{L'}{\kappa_i^2} = l_i \frac{2\sqrt{\pi}}{\Gamma(3/4)}\frac{\kappa_i}{\Delta\kappa'}, \qquad (12)$$

where the numerical factor $2\sqrt{\pi}/\Gamma(3/4) \approx 2.9$. The initially calculated value of the attenuation length l [Eq. (6)] and the result of an exact integration l' [Eq. (10)] normalized by l'' are given in Fig. 8 as functions of $\kappa/\Delta\kappa'$. One can see that for small values of the transverse wave number κ (i.e., for $\kappa \lesssim \Delta\kappa'/2$) the attenuation length can be approximated by l''. On the opposite end, for large values of κ ($\kappa \gtrsim \Delta\kappa'/2$), it corresponds to l with good accuracy. Light power in this region of nearly coaxial modes with $\kappa \lesssim \Delta\kappa'/2$ contributes to the central peak.

Where is the light power from the modes of this central peak scattered to? The profiles of the scattered power P_{sc} are given by the product $\rho(k_j)T_i(k_j)g(|k_j - k_i|)$, and for some typical initial mode wave numbers κ_i they are presented in Fig. 9(a). One can see that, even for the nearly coaxial modes, the maximum scattering occurs to the edge of the boundary region (at $\kappa \approx 0.8\Delta\kappa'$). Only 1/3 of the scattered power is left within the borders of the central peak [$\kappa \lesssim \Delta\kappa'/2$, see Fig. 9(b)], and the modes outside this region essentially do not return power into this central region [see the two middle curves of Fig. 9(a)].
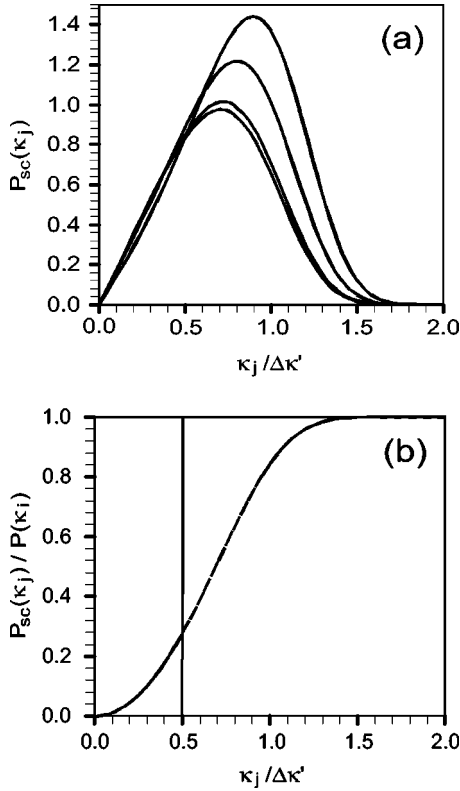
FIG. 9. (a) Profiles of the light power scattered from some modes of the central peak with transverse wave numbers $\kappa_i/\Delta\kappa'$ $\to 0, 0.2, 0.5$, and 0.7 (from the lowest to the uppermost curve). (b) Fraction of the light power scattered from nearly coaxial mode ($\kappa_i \to 0$) into the modes with $\kappa < \kappa_j$.

The next step is to show that the light power scattered in this way is dispersed via processes of intermode diffusion, and transferred rapidly to the other end of the allowed k region (at $k \to 1$) where it leaks from the waveguide through the side walls into the surrounding space. Let us suppose that the diffusion equation [Eq. (7)] is still valid down to the boundary of the central peak, i.e., down to $\kappa \approx \Delta\kappa'/2$. Numerical calculations performed using this equation (Fig. 10) for a typical value $\Delta\kappa' \approx 0.2$ predict a quite rapid (characteristic distance much shorter than L_D) dissipation of an initial Gaussian profile $\exp[-(\kappa - \Delta\kappa')^2/(\Delta\kappa'/2)^2]$. Indeed, the initial peak loses more that 50% of its initial amplitude after the
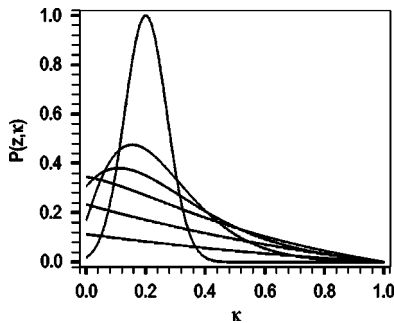
FIG. 10. Evolution of the initial mode distribution $\exp[-(\kappa -0.2)^2/(0.1)^2]$ as a result of propagation through different normalized waveguide lengths $z/L_D = 0, 0.05, 0.1, 0.2, 0.5$, and 1 (from the upper to the lower curve).

propagation length $z' \approx L_D/10$. By considering the possible influence of this process on backscattering into the initial ith mode one has also to take into account that only the modes that receive the power from this initial ith mode [see Fig. 9(a)] can deliver it back with the same efficiency as a result of similar scattering.

This result can also be supported by the following general arguments. If we consider the initial stage of dispersion of some narrow profile, and neglect the variations of the effective diffusion coefficient within it, our diffusion equation has the following Gaussian spreading solution (see also Refs. 25 and 26):

$$P(z,\kappa) = \frac{1}{\sqrt{z\kappa_0/L_D}}\exp\left[-\frac{(\kappa - \kappa_0)^2}{4z\kappa_0/L_D}\right]. \quad (13)$$

It follows from Eq. (13) that the characteristic length needed for a significant (i.e., by about a factor of 2) dispersion of such a narrow Gaussian power profile with an initial half-width $\Delta\kappa$ and centered at κ is approximately given by

$$z' \simeq L_D\Delta\kappa^2/\kappa. \quad (14)$$

Making the replacements $\Delta\kappa \simeq \Delta\kappa'/2$ and $\kappa = \Delta\kappa'$ reduces the above equation to

$$z' \simeq L_D\Delta\kappa'/4, \quad (15)$$

which corresponds to the results of the numerical calculations presented in Fig. 10 quite well.

Now we can compare the obtained characteristic dispersion length

$$z' \simeq \frac{da^2}{4n\delta^2}\frac{2\sqrt{n}}{\sqrt{ak_0}} = \frac{1}{8}\frac{da^{3/2}}{\sqrt{n}\delta^2\sqrt{k_0}}, \quad (16)$$

with the attenuation length [Eq. (12)] of a representative mode located at the boundary of the central peak region (i.e., one with $\kappa \approx \Delta\kappa'/2$),

$$l''(\Delta\kappa'/2) = \frac{d\sqrt{\pi n}\sqrt{a}}{4\Gamma(3/4)\delta^2 k_0^{3/2}}\frac{ak_0}{n} \approx 0.36\frac{da^{3/2}}{\sqrt{n}\delta^2\sqrt{k_0}}, \quad (17)$$

and see that the latter is nearly three times longer. This means that the intermode light diffusion is quite efficient in the unidirectional transfer of scattered power, even near the boundary of the central peak region. Because of the inverse quadratic dependence of l'' on κ [see Eq. (12)], l'' is definitely much larger than z' for internal modes of the central peak with smaller κ values.

This allows us to accept the following model for the dominating power transfer process in the region of the central peak: the initial power of every mode is scattered unidirectionally outside this area (in fact, to $\kappa \approx \Delta\kappa'$) from where light diffuses out to the opposite end of the allowed region of k values, and finally leaks into the surrounding space. This process of power out-diffusion is quite effective. No significant power is accumulated in the border area and, as a result, we can neglect backscattering of this light into the central peak. Since the power is scattered basically into the modes with $\kappa \gtrsim \Delta\kappa'/2$ [Fig. 9(a)] we can also neglect direct power exchange between modes of the central peak.

The efficiency of such unidirectional light scattering is strongly κ dependent [see Eq. (12)], and this determines the distribution of power within the central peak. Indeed, let us assume that the central peak region was initially excited by some uniform distribution of the input light density $P(0,\kappa) = P_0(\text{const}(\kappa))$. As a result of scattering the initial power of every mode decreases exponentially in accordance with its corresponding characteristic attenuation length $l''(\kappa)$

$$P(z,\kappa) = P_0 \exp\left[-\frac{z}{l''(\kappa)}\right] = P_0 \exp\left[-\left(\frac{\kappa}{\kappa_0}\right)^2\right], \quad (18)$$

where

$$\kappa_0 = \sqrt{L'/z} \approx 0.60 \sqrt{\frac{dn^{1/2}a^{1/2}}{\delta^2 k_0^{3/2}z}}. \quad (19)$$

Since $\theta \approx \kappa$ in the region of the central peak, one can see that a Gaussian angular power profile is shaped from the initial uniform distribution. The characteristic radius of this profile (κ_0) decays slowly with the propagation distance ($\propto z^{-1/2}$). As long as we can neglect the discrete mode structure (i.e., when κ_0 is much bigger than the intermode distance π/dk_0), the amplitude of the central maximum of the profile is constant.

The above results [and in particular the final equations (18) and (19)] were obtained for the model case of a 1D slab waveguide. However, one can show that they differ little from those for a multimode optical fiber (i.e., a 2D dielectric waveguide with cylindrical cross section) with 2D surface roughness. Indeed, the basic relation for the transmittance coefficient represented by Eq. (3) is practically the same for a multimode 1D slab waveguide and a multimode optical fiber (see, e.g., Refs. 22 and 24).

The intermode power diffusion equations that are obtained for these two cases[22] are a little bit different in their structure. However, the result for the dispersion of a narrow Gaussian profile, Eq. (13), is the same. As a result, the main remaining difference in the calculations of the attenuation length l'' is associated with the necessity of summing (or integrating) over the radial m and azimuthal l mode indices of the final modes in the scattering process (see the permitted mode indices diagram[24] in Fig. 11).

Under the assumption that the fiber surface roughness has the same statistical properties along the z direction (fiber axis) and along the orthogonal one, the area of the final modes that participate effectively in the scattering from the fundamental mode (i.e., coaxial, with $m=1, l=0$), is elongated along the m axis (Fig. 11). Unlike the summation over the radial mode index, which is similar to that performed above for the 1D slab, the summation over the final mode azimuthal index can be replaced, with good accuracy, by integration over the corresponding roughness components with integration limits $\pm\infty$. As one can see from the diagram this is not correct for processes whose final radial mode indices are very small, but they play a minor role in the diffusion process (see Fig. 9). However, if one can replace summation over the azimuthal mode indices by integration over the corresponding roughness components with integration limits $\pm\infty$, the summation over all the possible final modes reduces to summation over only the radial mode indices (see,
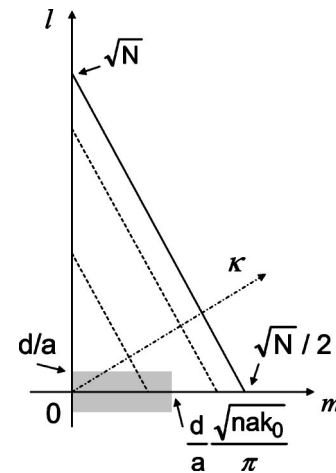
FIG. 11. "$l-m$" diagram for the optical fiber, showing the triangular region of permitted guided mode indices. The parallel dashed lines show mode groups with fixed transverse wave number κ. The rectangle shows the effective area of the final modes for scattering from the fundamental mode with $m=1$ and $l=0$ (N is the total number of modes supported by the fiber).

e.g., Ref. 22). As in the case of a 1D slab, this can be replaced by integration over the transverse κ (or longitudinal k) wave numbers of the final mode, which will lead to exactly the same final results.

IV. DISCUSSION

According to the theoretical analysis presented above, one of the most prominent consequences of having ballistic transport of light in the modes with small wave numbers κ of a roughened optical fiber is the formation, through propagation, of a narrow angular distribution of power around the axial mode. This, in turn, gives rise to the narrow angular intensity distribution emerging from the fiber that was observed in our experiments. When the modes of the corrugated fiber are excited with a more or less uniform angular distribution, as shown in Fig. 3, the distribution evolves into a Gaussian-like profile [see the inset of Fig. 4(a)] quite rapidly. Even for initial profiles with a doughnutlike shape, the final distribution is the same (Fig. 6).

The theoretical analysis also indicates that the axial intensity should be invariant upon propagation [see Eq. (18)], and our experimental observations agree with this prediction quite well [Fig. 4(b)]. This is associated with the simple fact that the efficiency of all power transfer processes for the coaxial modes (i.e., those with small mode index) tends to zero as the number of propagating modes grows. The only fundamental reason that can lead to some attenuation of the transmitted power in the center of the angular profile is that some finite transverse wave number $\kappa_{min} \approx \lambda/2d$ can also be attributed even to the fundamental, coaxial mode. This effect is, however, too weak to be observed under the conditions of our experiments.
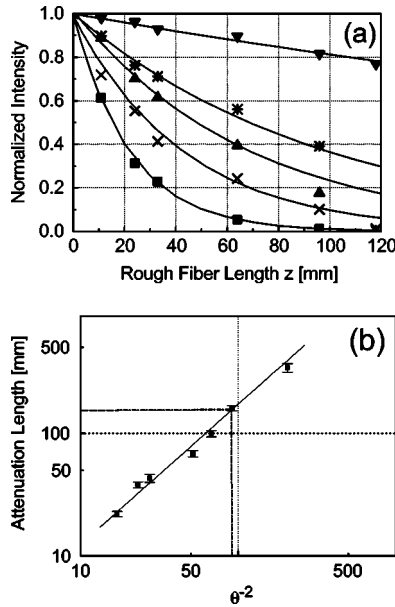
FIG. 12. (a) The attenuation of the transmitted intensity for different modes as a function of the propagation length for angles of observation $\theta = 4°(\blacktriangledown), 7°(*), 8°(\blacktriangle), 11°(\times),$ and $14°(\blacksquare)$; the solid lines show the corresponding exponential fits. (b) The attenuation length as a function of the inverse square of the mode output angle; the solid line shows the slope corresponding to a θ^{-2} dependence.

The propagating Gaussian profile is characterized by a slowly reducing width $\Delta\theta(z)$ for which our theoretical analysis [Eq. (19)] predicts an inverse square root dependence [$\Delta\theta(z) \propto 1/\sqrt{z}$]. The experimental data [Fig. 4(a)] can be fitted reasonably well with this kind of dependence. The formation of the Gaussian angular profile is associated with a quadratic transverse wave number dependence ($\propto \kappa_i^2$) for the efficiency of scattering between modes within the central maximum [see Eq. (12)]. This kind of dependence is in agreement with the experimental data obtained using a selective excitation of modes (Fig. 6). Indeed, from the experimental data represented by Fig. 6(a), which correspond to a relatively flat profile of excitation, one can evaluate the decay rate of the power transmitted through the fiber and observed at different scattering angles ($\theta = 4°, 7°,$ and $8°$). With reasonable accuracy the decay can be fitted by an exponential function [Fig. 12(a)], which is typical for ballistic transport.

For the incidence angles $\theta_{in} = 10°$ and $15°$ [Figs. 6(b) and 6(c)] we also observe an exponential decay of transmitted power for modes corresponding to the initially excited ones [see corresponding curves in Fig. 12(a) obtained for $\theta = 11°$ and $14°$]. In contrast, modes with smaller propagation angles (i.e., those located inside the initially excited ring) maintain a practically constant power until the disappearance of the initially excited ring distribution. Only after this, does one have the relatively fast attenuation observed in Fig. 6(a). We attribute this effect to an efficient power transfer from the ring maxima into the internal modes with smaller propagation angles. Obviously, these more complicated conditions of the power exchange are not suitable for the evaluation of the scattering efficiency of the modes located inside the central area.

The characteristic decay length of the mode power as a function of θ^{-2}, obtained from Fig. 12(a), is presented in Fig. 12(b) on a log-log scale. Plotted in this way, the data fit quite well an inverse quadratic dependence predicted by Eq. (12). The absolute value of the attenuation length (e.g., ≈ 160 mm for $\theta = 6°$) also allows us to estimate the characteristic attenuation length L' as ≈ 1.6 mm. Employing the typical surface parameters $a \approx 5$ μm and $\delta \approx 0.06$ μm, we can also evaluate this parameter from Eq. (12) as $L' \approx 1.5$ mm. Bearing in mind the simplicity of the theoretical model used above, this correspondence between the experimentally measured value of L' and its theoretical estimate is a good one.

V. SUMMARY AND CONCLUSIONS

In summary, we have presented experimental results on the transmission properties and the power exchange between the modes of a multimode optical fiber with rough surfaces. We have shown that, irrespective of the initial conditions of excitation of the fiber, the angular power distribution finally evolves into a Gaussian-like shape that propagates with a slowly reducing width. It was also observed that for each mode and as a function of the propagation distance the transmitted power presents an exponential decay whose characteristic attenuation length decays quadratically with the mode propagation angle.

The experimental results are accompanied by a theoretical analysis of the incoherent intermode power exchange in a 1D slab waveguide, based on a continuous mode distribution approximation. It was shown that, under typical conditions, the guided modes of the central peak (i.e., those with low index numbers) obey the predictions of a ballistic propagation model. The simple model employed explains the evolution of an initial uniform power distribution into a Gaussian-like angular power profile. The analysis also explains the experimentally observed dependence of the mode attenuation length with the mode index, and the slow (inverse square root dependence on the propagation distance) reduction of the angular width of the Gaussian-like profile. While the theoretical analysis is based on the assumption of a 1D slab waveguide, it is argued that the results obtained are also valid for a multimode optical fiber with a 2D surface corrugation. The characteristic attenuation lengths of the modes, evaluated from the roughness parameters of the fiber surface measured by the profilometer, proved to be in reasonable agreement with those observed experimentally.

It should be noted that due to the strong leakage of light into surrounding space the scattering system we studied here is an open one. This fact makes difficult the observation of localization effects in the experiments described.

*On leave from División de Física Aplicada, Centro de Investigación Científica y de Educación Superior de Ensenada, Apartado Postal 2732, Ensenada, Baja California, 22800, Mexico.

[1] D. Marcuse, Bell Syst. Tech. J. **48**, 3187 (1969).

[2] J. T. Boyd and D. B. Anderson, IEEE J. Quantum Electron. **QE-14**, 437 (1978).

[3] E. Bradly and D. G. Hall, Opt. Lett. **7**, 235 (1982).

[4] P. Mazur and D. L. Mills, J. Appl. Phys. **54**, 3735 (1983).

[5] M. E. Lines, J. Appl. Phys. **55**, 4052 (1984).

[6] S. John, H. Sompolinsky, and M. J. Stephen, Phys. Rev. B **27**, 5592 (1983).

[7] M. Kaveh, Philos. Mag. B **56**, 693 (1987).

[8] P. Shen, *Introduction to Wave Scattering, Localization and Mesoscopic Phenomena* (Academic Press, New York, 1995).

[9] D. S. Wiersma, P. Bartolini, and Ad. Lagendijk, Nature (London) **360**, 671 (1997).

[10] A. Z. Genack and N. Garcia, Phys. Rev. Lett. **66**, 2064 (1991).

[11] M. S. Stoytchev and A. Z. Genack, Opt. Lett. **24**, 262 (1999).

[12] V. Tripathi and D. E. Khmelnitskii, Phys. Rev. B **58**, 1122 (1998).

[13] Y. M. Blanter, A. D. Mirlin, and B. A. Muzykantskii, Phys. Rev. Lett. **80**, 4161 (1998).

[14] J. A. Sanchez-Gil, V. Freilikher, I. Yurkevich, and A. A. Maradudin, Phys. Rev. Lett. **80**, 948 (1998).

[15] A. García-Martin, J. A. Torres, J. J. Sáenz, and M. Nieto-Vesperinas, Appl. Phys. Lett. **71**, 1912 (1997).

[16] A. García-Martin, J. J. Sáenz, and M. Nieto-Vesperinas, Phys. Rev. Lett. **84**, 3578 (2000).

[17] J. A. Sánchez-Gil, V. Freilikher, A. A. Maradudin, and I. Yurkevich, Phys. Rev. B **59**, 5915 (1999).

[18] J. A. Sanchez-Gil and V. Freilikher, Phys. Rev. B **67**, 075103 (2003).

[19] F. M. Izrailev and N. M. Makarov, Opt. Lett. **26**, 1604 (2001).

[20] E. I. Chaikina, N. Puente, T. A. Leskova, and E. R. Méndez, Proc. SPIE **4447**, 122 (2002).

[21] E. I. Chaikina, S. Stepanov, T. A. Leskova, E. R. Méndez, and A. G. Navarrete, Proc. SPIE **5189**, 50 (2003).

[22] S. Stepanov, E. I. Chaikina, T. A. Leskova, A. G. Navarrete, and E. R. Méndez, J. Opt. Soc. Am. A (to be published).

[23] V. Riuz-Cortéz, E. R. Méndez, Z. H. Gu, and A. A. Maradudin, Proc. SPIE **1558**, 222 (1991).

[24] D. Marcuse, *Theory of Dielectric Optical Waveguides*, 2nd ed. (Academic Press, San Diego, 1991).

[25] F. G. Bass, V. D. Freilikher, and I. M. Fuks, IEEE Trans. Antennas Propag. **AP-22**, 288 (1974).

[26] F. G. Bass and I. M. Fuks, *Wave Scattering from Statistically Rough Surfaces* (Pergamon Press, New York, 1979).